Journal Section *Behavioral/Systems/Cognitive*

Common or redundant neural circuits for duration processing across audition and touch.

Abbreviated title: Somatosensory and auditory duration processing

John S. **Butler**[1,2], Sophie **Molholm**[1,2], Ian C. **Fiebelkorn**[1,2], Manuel R. **Mercier**[1,2,3],

Theodore H. **Schwartz**[3] and John J. **Foxe**[1,2]

[1]The Cognitive Neurophysiology Laboratory
Children's Evaluation and Rehabilitation Center (CERC)
Departments of Pediatrics & Neuroscience
Albert Einstein College of Medicine
1225 Morris Park Avenue
Bronx, New York 10461, USA

[2] The Cognitive Neurophysiology Laboratory
Program in Cognitive Neuroscience
Departments of Psychology & Biology
The City College of New York
138th Street and Convent Avenue
New York, New York 10031, USA

[3] Department of Neurological Surgery
Weill Cornell Medical College
New York Presbyterian Hospital,
525 East 68th Street
New York, New York 10021, USA

Correspondence:
Prof. John J. Foxe
Departments of Pediatrics & Neuroscience
Albert Einstein College of Medicine

1225 Morris Park Avenue
Bronx, NY 10461
Email: john.foxe@einstein.yu.edu

17 Pages, 3 Figures, 0 Tables, 2 Equations, 244 words in abstract, 587 words in the introduction, 1,281 words in the discussion

Keywords: Somatosensory, Auditory, duration processing, mismatch negativity, multisensory, cross-modal

Supplementary Material

DIPOLE SOURCE ANALYSIS

Methods

To estimate the location of the intra-cranial generators of the scalp recorded grand mean MMNs, we performed source modeling using brain electric source analysis (BESA 5.1.8, MEGIS Software GmbH, Gräfelfing, Germany; Scherg and Von Cramon, 1985). BESA employs a least-squares fitting algorithm, defining location and orientation of dipoles for which the maximal amount of variance is explained (see Scherg and Picton, 1991; Simpson et al., 1995). For the purpose of modeling, an idealized four-shell ellipsoidal head model with a radius of 90 mm and scalp and skull thickness of, respectively, 6 and 7 mm is assumed. It should be noted that dipole modeling only provides a center of mass of the loci of the generators underlying a specific scalp distribution and therefore the specific brain coordinates should not be taken literally.

We took two approaches to modeling the data. The first was to fit the location of symmetrically placed dipoles on the basis of prior knowledge of the loci of the MMN generators. This is referred to as a seeded fit. The other approach was to allow a pair of symmetrically constrained dipoles to freely fit the data. The latter allowed us to determine 1) if a free fit would greatly improve the seeded fit and therefore better account for the data, and 2) to assess the validity of the seeded fit: If it resulted in the similar placement of the dipoles (i.e., in the vicinity of auditory cortex for the aMMN and in the vicinity of somatosensory cortex for the sMMN), this would provide additional support for the seeded models. The windows of analysis for the early and late components were from 126 to 166ms and 210 to 250ms, respectively, for both MMNs. The best fit within the window of analysis is reported.

aMMN:

seeded fit: For each of the early and late MMN responses, a pair of dipoles was seeded based on the loci of the intracranial contacts where the duration aMMN was seen in the current study, and based on data from a previous study from our laboratory in which fMRI was used to localize the duration aMMN (Molholm et al., 2005). From these the placement of the dipoles was fixed in the Superior Temporal Gyri (STG; MNI: -58,-24, 8/58, -24, 8, Figure S1 Left). The orientation of the dipoles was allowed to freely rotate. For the early and late component this yielded a goodness-of-fit of 76% and 90%, respectively, indicating that this placement could account for the majority of the signal, especially for the later window where the signal was considerably larger. The addition of a pair of symmetrically constrained dipoles that were allowed to freely fit improved the early and late solutions each by 7%. The early component dipoles localized to the middle frontal gyrus, Brodmann's area 9. The late component dipoles localized to the cingulate gyrus in frontal cortex, Brodmann's area 32.

free fit: A fully free-fit model was also applied to determine if this provided a stronger source modeling solution. For the early component the free-fit model resulted in a goodness-of-fit of 78%, with the dipoles located just superior to the STG, in Brodmann's area 13 of the postcentral gyrus (MNI; 49, -9, 11/ -49, -9, 11). Adjusting the placement slightly so that the dipoles were in the STG, the fit remained at 78%. For the late component the free-fit model resulted in a goodness-of-fit of 96%, with the dipoles located at MNI:-27,-24, 44/27,-24, 44 (Frontal Lobe, Sub-Gyral, White Matter). Adjusting these to the closest region in the STG, the fit remained at 96%.

Both the seeded and the fixed solutions provide good fits for the data, with the majority of the variance accounted for by placements in auditory cortex.

sMMN:

seeded fit: A pair of dipoles was seeded in the postcentral gyri (PcG; MNI: -35,-30, 57/35, -30, 57), corresponding to where we observed the duration sMMN in the intracranial data, and orientation was allowed to freely fit. This yielded a goodness-of-fit for the early and late component of 77% and 87%, respectively (Figure S1 Right), indicating that this model could account for the majority of the signal. The addition of a pair of symmetrically constrained dipoles that were allowed to freely fit improved the early solution 8% and the late solution by 3%. For the early component the additional dipoles were localized outside of brain space; adjustment to the nearest brain region resulted in placement in visual cortex (BA17), in the posterior occipital lobe, Brodmann's area 17. For the late component the dipoles settled in subgyral white matter in the frontal lobe. Because this placement was not sufficiently near grey matter and because it did not greatly affect the goodness of fit, we do not consider it meaningful.

free fit: A fully free-fit model was also applied for comparison. For the early component free-fit dipole resulted in a goodness-of-fit of 76.7%, with the dipoles located in Brodmann's area 5 of the precentral gyrus (MNI; -16, -38, 44/ 16, -38, 44).

The late component free-fit dipole resulted in a goodness-of-fit of 91%, with the dipoles located in Brodmann's area 4 of the precentral gyrus. Adjusting the placement slightly so that the dipoles were in somatosensory cortex (MNI:-24, -34, 53/24, -34, 53) resulted in a fit of 89%.

Thus for the sMMN, both the seeded and the free-fit solutions provide good fits for the data (although the free-fit solution required adjustment from motor to nearby somatosensory cortex).

Conclusions: The results from dipole modeling of the MMN data are consistent with the thesis that duration processing occurs in sensory specific cortex for auditory and somatosensory stimuli. The models provided excellent fits of 76% or greater, especially when it is considered that these were conducted on the derived difference waves. Adding additional sources (dipoles) did not result in localization of a common source across the aMMN and sMMN models, or in consistent placement for the early versus the late aMMN or sMMN.

Figures S1 and S2 present dipole source solutions for the aMMN and sMMN, respectively. All dipole solutions consisted of two dipoles constrained to be symmetric in position.

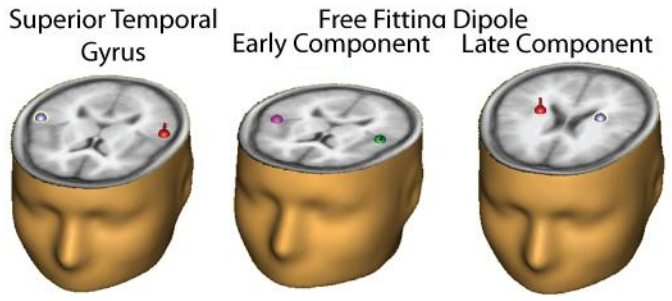

Figure S1 The dipolar solutions of the grand mean aMMN component. Left: seeded model Right: free-fit model.

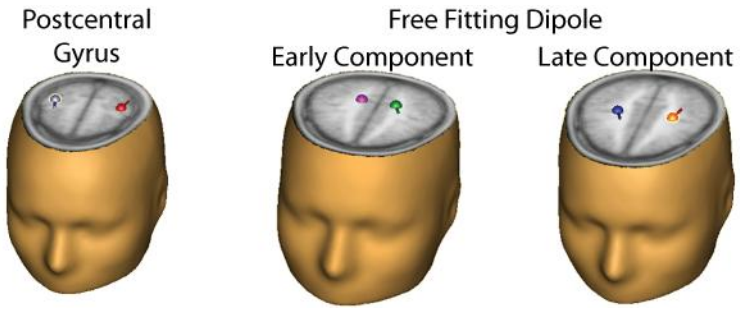

Figure S2 The dipolar solutions of the grand mean sMMN component. Left: seeded model Right: free-fit model

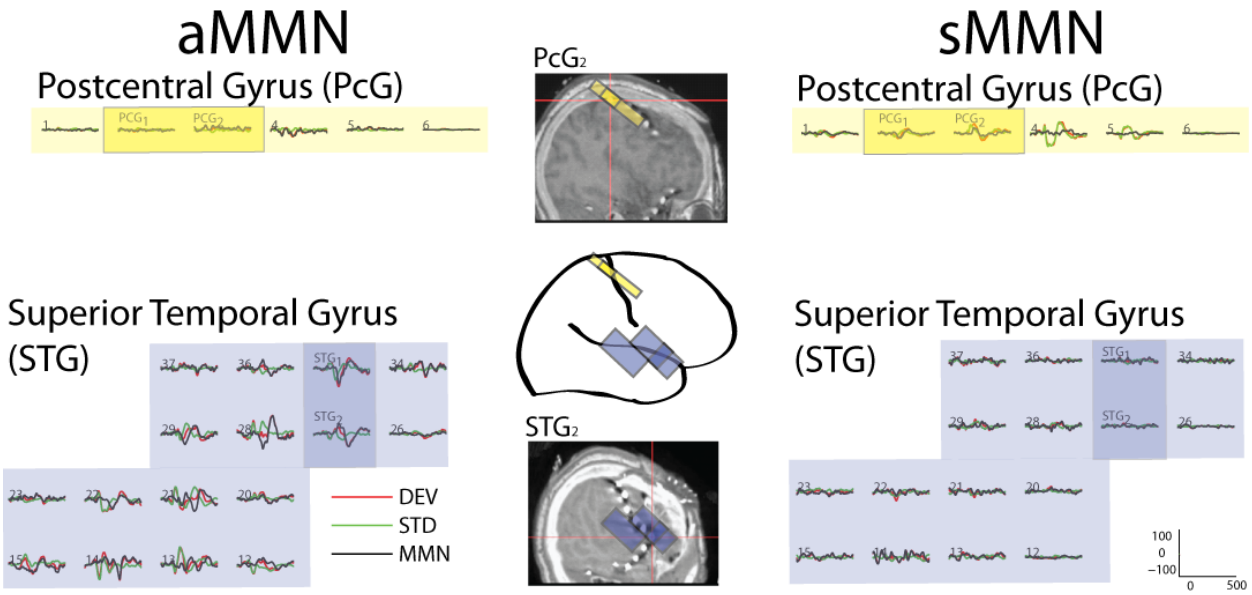

Figure S3. Responses at 22 intracranial sites along the postcentral gyrus and the superior temporal gyrus are depicted. The left and right columns show the aMMN and sMMN conditions, respectively. The top row of responses corresponds to the strip located along the postcentral gyrus. These are shaded yellow, with the corresponding locations shaded similarly on the depiction of the brain. The bottom set of responses represents a subset of the grid covering the region of the Sylvian fissure. These are shaded purple, with the corresponding locations shaded similarly on the depiction of the brain. The darker purple and yellow shading indicates those electrode sites reported in the main text. For illustrative purposes, the approximate locations of the electrode grids are projected onto a cartoon rendering of the brain. The actual anatomical locations of the contacts of interest are illustrated here in the two panels depicting CT-MRI reconstructions, and in similar reconstructions in Figure 3 of the main text.

References

Molholm S, Martinez A, Ritter W, Javitt DC, Foxe JJ (2005) The neural circuitry of pre-attentive auditory change-detection: an fMRI study of pitch and duration mismatch negativity generators. Cereb Cortex 15:545-551.

Scherg M, Picton TW (1991) Separation and identification of event-related potential components by brain electric source analysis. Electroencephalogr Clin Neurophysiol Suppl 42:24-37.

Scherg M, Von Cramon D (1985) Two bilateral sources of the late AEP as identified by a spatio-temporal dipole model. Electroencephalography & Clinical Neurophysiology, 62:32-44.

Simpson GV, Foxe JJ, Vaughan HG, Jr., Mehta AD, Schroeder CE (1995) Integration of electrophysiological source analyses, MRI and animal models in the study of visual processing and attention. Electroencephalogr Clin Neurophysiol Suppl 44:76-92.